Chapter 4

Multifractality in ^{32}S-Ag/Br interaction at 200A GeV/c

The multifractal structure of nonstatistical fluctuations in the phase-space distribution of singly charged particles produced in ^{32}S-Ag/Br interactions at an incident momentum of 200A GeV/c has been investigated. Various parameters related to multifractality have been obtained by analysing the data. Besides obtaining the fractal dimensions and a smooth multifractal spectrum, the experimental results have also been used to determine universal parameters like the Levy index, and the multifractal specific heat. The experimental results have been compared with those obtained from an event sample simulated by the Lund Monte Carlo code FRITIOF.

4.1 Introduction

We have already seen that the single particle distribution of secondary charged particles produced in a ^{32}S-Ag/Br interaction at 200A GeV/c, exhibits rapid fluctuations containing both sharp peaks and deep valleys in the phase-space density (dn_s/dX) values. It has also been mentioned that, these fluctuations result both from the statistical noise due to finite multiplicity of particles in an event, as well as from some dynamical reason that is not directly accessible to any experiment. The extent of such fluctuations depends on the resolution at which the density distribution is analyzed. Effects of statistical noise can be substantially reduced by taking an average over a large number of events. While doing so, unfortunately the dynamical components too are averaged out resulting in a smooth distribution of final state hadrons, as can be found in Fig. 2.3. Making use of suitable data analysis techniques characteristics of the dynamical component can still be investigated, and the mechanism of multiparticle production can be explored within the framework of existing models. One such set of techniques is based on the notion that the density fluctuations have self-similar multifractal property, that probably is an outcome of some kind of scale invariant dynamics. The fluctuation properties can be quantified by evaluating appropriate multifractal moments of the distribution, and by examining how they depend on the phase-space interval size, say δX. It has been suggested in theory [1–3] and observed in experiments [4–8] that, self-similarity in density fluctuations should lead to a power law scaling behaviour of δX dependence of the multifractal moments. Such scaling laws can further be utilized to extract universal fractal properties of the underlying distribution and its fluctuation. Efforts have been made to interpret the observed scale invariance in terms of random cascading model, phase transition or more conventional phenomenon like the Bose-Einstein correlation; but each with limited degree of success. Both the experimental and phenomenological status of the subject have been comprehensively reviewed in [9].

In Chapter III dynamical fluctuations have been analyzed in terms of the intermittency phenomenon. In this technique the scaled factorial moments (SFMs) of different order are evaluated. In one dimension the event space averaged SFM $< F_q >$ of order q has been found to scale with δX following

$$< F_q > \propto \delta X^{-\phi_q}, \tag{4.1}$$

where ϕ_q is called the intermittency index. This self-similarity of fluctuations in the density of produced particles down to the experimental resolution indicates that, fractal structures are involved in the process of particle emission. Though the SFMs are very efficient to suppress Poisson type noise, they do suffer from a few limitations as well. For example, the order q must always be a positive integer - it can neither be a fraction nor a negative number. The SFM provides information only about the peaks in particle density, but the technique is not suitable for analyzing the dips or valleys in the distribution. It's therefore quite natural to extend the scope of investigation beyond intermittency, to verify a probable existence of interrelated fractal characteristics in the already used ^{32}S-data, and also to find out interpretation of the intermittency parameters in terms of the fractal parameters. In this chapter we have therefore, presented some results on multifractal analysis of the density fluctuation of singly charged produced particles in ^{32}S-Ag/Br interactions at 200A GeV/c. In particular, the scaling behaviour of multifractal moments as functions of δX has been examined by using two different techniques [1, 11, 12] to be described later. Results obtained from these two different formalisms have been compared to the extent possible. ^{32}S-Emulsion interactions at 200A GeV/c have been simulated by using the computer code FRITIOF based on the Lund Monte Carlo model [13] on high energy AB interaction. Results obtained by analyzing a sample of FRITIOF generated ^{32}S-Ag/Br events, having identical multiplicity distribution of produced particles as the experimental one, have been compared with experimental results. The main objectives of this chapter are therefore, (i) to establish the presence of multifractal characteristics in the experimental data beyond those arising from trivial statistical noise, (ii) to extract relevant fractal parameters that can help develop future models of particle production, (iii) to see whether or not FRITIOF can reproduce the experimentally observed results, and finally (iv) to examine how the results obtained from two different multifractal techniques adopted in this investigation, agree or disagree with each other.

4.2 Hwa's Multifractal Moments

Scale invariance of fluctuations in the density distribution of final state hadrons, as observed from the intermittency analysis of the present set of data [10] indicates that, with

the help of fractal geometry it may also be possible to characterize the distribution. According to the theory of multifractality the number density of final state hadrons should scale with the phase-space partition size, and the scaling properties should be different in different regions of phase-space. Unlike a geometrical or a statistical system, multiparticle production process possesses special problems, the most obvious one being the finiteness of average shower track multiplicity $< n_s >$. For finite $< n_s >$ the frequency distribution and its moments are subjected to large statistical fluctuations. As the bin size gets smaller, the problem of statistical noise arising out of growing presence of empty bins requires special attention. The multifractal moment (G-moment) of order q, also known as the frequency moment, is defined for an event as

$$G_q = \sum_{j=1}^{M} (p_j)^q = \sum_{j=1}^{M} \left(\frac{n_j}{n_s}\right)^q, \tag{4.2}$$

where q is any (+)ve or (-)ve real number, when the entire phase-space interval, say ΔX, has been divided into M equal intervals and n_j is the number of particles in jth such interval. In the above expression two points are to be noted, (i) the summation runs only over nonempty intervals ($n_j \neq 0$) allowing negative values of q, and (ii) for finite n_s, however large, p_j can not represent the true probability, but at the best may be called a relative frequency. For negative q the G-moments are capable of providing information about dips in the phase-space distribution.

By definition, a fractal dimension D_F relates the mass element (δm) of an object having fractal characteristics to its size, say δl, through

$$\delta m \sim [\delta l]^{D_F}.$$

For ordinary objects D_F equals the topological dimension D of the supporting space, whereas for fractal objects they do not. At small δl the probability $p(\delta l)$ to be within a hypervolume may be assumed to scale with its size,

$$p(\delta l) \propto [\delta l]^{D_F} : \quad D_F = \text{constant},$$

and therefore, for a fractal object the mean qth order moment should abide by,

$$< p(\delta l)^q > \propto [\delta l]^{q\,D_F}.$$

In the theory of multifractal structure of particle distribution this notion of fractal theory has been generalized as,

$$G_q = \sum_{j=1}^{M} p_j^q(\delta X) = \left\langle p_j^{q-1}(\delta X) \right\rangle \propto (\delta X)^{\tau(q)}, \tag{4.3}$$

where $\tau(q) = (q-1)\, D_q$ and D_q is called the Renyi dimension. In stead of fractal dimension, a multifractal may also be characterized by a spectral function. Each phase-space interval has its own δX dependence. If all singularities associated with a particular scaling index α (may be termed as the local mass dimension in the sense, $p_j(\delta X) \sim (\delta X)^{\alpha}$: $\delta X \to 0$) are grouped together to form a fractal subset $S(\alpha)$, then the number of intervals to fill up $S(\alpha)$ may be assumed to increase with decreasing δX as,

$$M_\alpha(\delta X) \sim (\delta X)^{-f(\alpha)},$$

where $f(\alpha)$ is the fractal dimension for $S(\alpha)$. Since each $S(\alpha)$ is associated with a particular α the summation in G_q over j may be replaced by,

$$\sum_{j=1}^{M} \to \int d\alpha\, \rho(\alpha)(\delta X)^{-f(\alpha)},$$

where $\rho(\alpha)$ is some weight factor whose exact analytic form is not very important. Thus at small δX,

$$G_q \propto \int d\alpha\, \rho(\alpha)(\delta X)^{-f(\alpha)+q\alpha},$$

and the dominant contribution comes from the region where the exponent is small. For each q, the minimum in the exponent occurs at a particular α say at $\alpha = \alpha_q$, that may be determined by setting,

$$\frac{d}{d\alpha}\left[q\alpha - f(\alpha)\right] = 0,$$
$$\frac{d^2}{d\alpha^2}\left[q\alpha - f(\alpha)\right] < 0.$$

Therefore, it suffices to evaluate the integral at or around α_q, when

$$\frac{d}{d\alpha_q} f(\alpha_q) = q \quad \text{and} \quad \frac{d^2}{d\alpha^2} f(\alpha_q) < 0.$$

From Eq. (4.3) we therefore get,

$$\alpha_q = d\tau(q)/dq$$

and

$$\tau(q) \approx q\alpha_q - f(\alpha_q).$$

The effect of empty bins has been taken care of by defining a modified form of the multifractal moment for a single event as [11],

$$G_q = \sum_{j=1}^{M} \left[\frac{n_{ij}}{(n_s)_i}\right]^q \Theta(n_{ij} - q). \tag{4.4}$$

Here n_{ij} is the number of particles in the jth bin of the ith event, $(n_s)_i$ is the total number of particles in the ith event, $\left[(n_s)_i = \sum_{j=1}^{M} n_{ij}\right]$, and Θ is a step function for integer as well as fractional q as defined in [11]. As mentioned above in the theory of fractals, if self-similar dynamical component is present in the density fluctuation, the G-moments should exhibit a scaling behaviour like,

$$G_q(\delta X_\eta) \propto M^{-\tau(q)} : \quad \delta X_\eta \to 0. \tag{4.5}$$

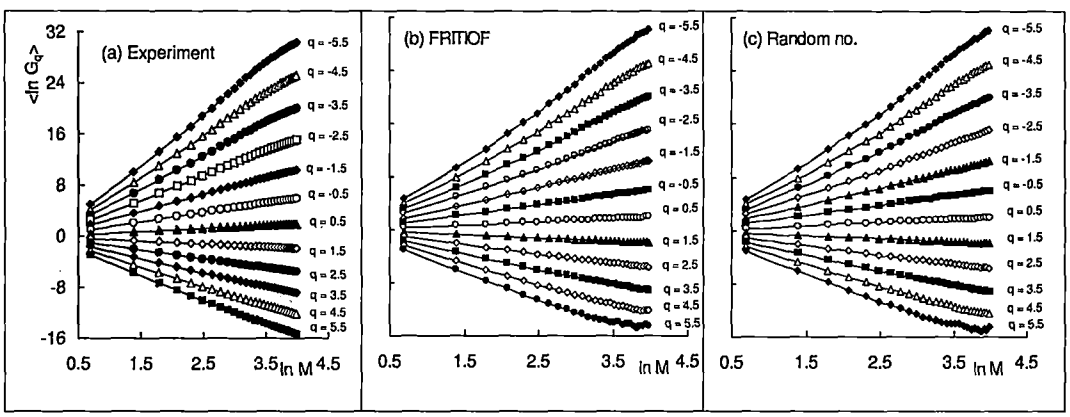

Figure 4.1: Variation of G-moments with phase-space partition number for ^{32}S-Ag/Br interaction at 200A GeV/c - (a) Experiment, (b) FRITIOF and (c) Random number. In all diagrams the continuous lines are drawn simply by joining the points.

Here $\tau(q)$ may be called the mass exponent. As long as M remains finite, the limit $\delta X_\eta \to 0$ can not actually be reached and, therefore, the fractal behaviour can not be extracted in its strict sense. However, by examining the scaling properties of the G-moments in a region where δX_η is of the order of the phase-space resolution permitted by the experiment, significant results can still be obtained. Taking the vertical average of

G-moments over the sample of events under consideration, one can determine the event space average of the mass exponent as,

$$< \tau(q) >= -\frac{\partial(< \ln G_q >)}{\partial(\ln M)}. \tag{4.6}$$

The methodology summarized above and as described in [1, 2, 11] allows us to determine various parameters related to multifractal characteristics of density fluctuation. Values of $< \ln G_q >$ for different q have been graphically plotted against $\ln M$ in Fig. 4.1. The experimental results, the FRITIOF simulated results and the results obtained by random number generation are shown separately. In general, for all three sets of data $< \ln G_q >$ linearly depends on $\ln M$ in accordance with Eq. (4.5), increasing for $q < 0$ and decreasing for $q > 1$. However, in the large $\ln M$ region saturation effects, due to finiteness of $< n_s >$, are visible particularly at high $|q|$. Following Eq. (4.6) the $< \tau_q >$ values can be determined for each q from the best linear fit of the $\ln M$ dependence of $< \ln G_q >$.

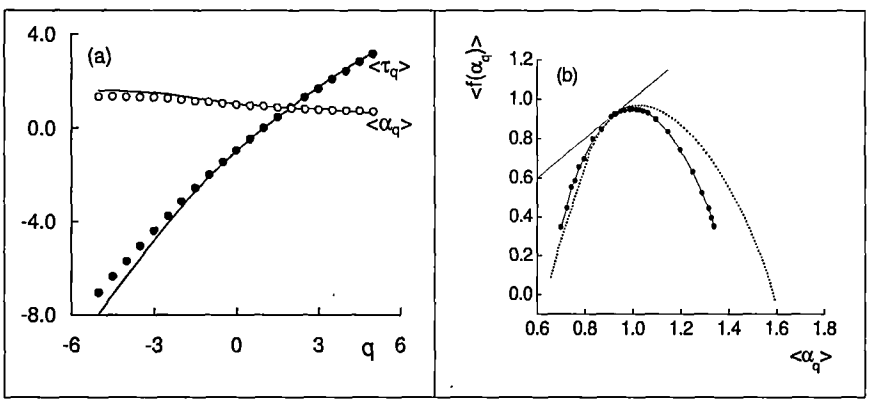

Figure 4.2: (a) Event averaged mass exponents $< \tau_q >$ and Lipschitz-Holder exponents $< \alpha_q >$ against q for ^{32}S-Ag/Br interaction at 200A GeV/c. Data points represent the experimental values and the lines represent the corresponding FRITIOF predictions. (b) Multifractal spectral function for both the experiment and FRITIOF. The solid curve with points represents experimental results and the dotted curve represents the FRITIOF prediction. The straight line represents $< f(\alpha_q) >=< \alpha_q >$.

The event space averaged multifractal spectral function

$$< f(\alpha_q) >= q < \alpha_q > - < \tau(q) >,$$

is introduced through a Legendre transform with the help of Lipschitz-Holder exponent α_q, that is defined as,

$$< \alpha_q >= \partial < \tau(q) > /\partial q.$$

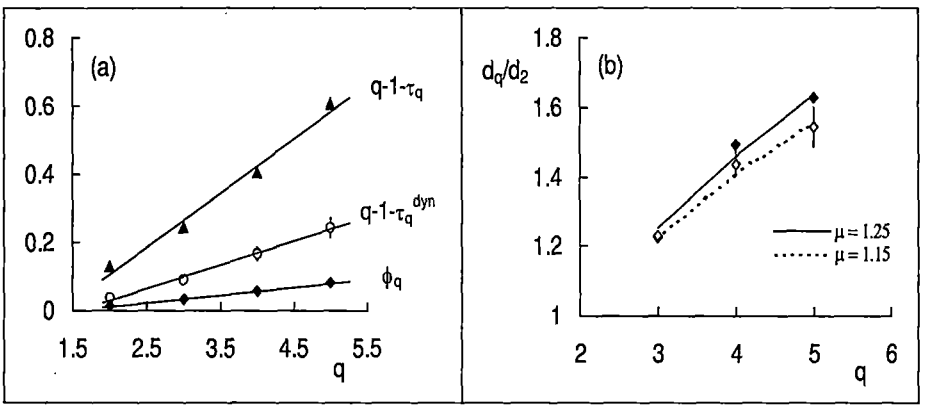

Figure 4.3: (a) Experimental values of the intermittency indices (ϕ_q), ($q - 1 - < \tau(q) >$) and ($q - 1 - < \tau(q) >^{dyn}$) are plotted against q for ^{32}S-Ag/Br interaction at 200A GeV/c. The straight lines are best linear fit to data. (b) Experimental values of d_q/d_2 obtained both from SFM (solid diamonds) and G-moments (open diamonds) are plotted against q. The continuous (solid and dotted) lines represent the corresponding Levy law prediction using Eq. (4.11).

Since a derivative is involved, it is necessary to determine $< \alpha_q >$ for small incremental changes in q, especially in the neighbourhood of $q = 0$, where $< f(\alpha_q) >$ has its maximum. In Fig. 4.2(a) we have shown how $< \tau_q >$ and $< \alpha_q >$ values for the experimental and FRITIOF data vary with q. Unlike in the case of intermittency analysis [10], we do not see any significant difference between the experimental and simulated results from multifractal analysis. A smooth and stable multifractal spectral function $< f(\alpha_q) >$ has been obtained both for the experiment and for the FRITIOF. Both of them are plotted against $< \alpha_q >$ in Fig. 4.2(b), and both satisfy the general characteristics [1, 3] such as, (i) $< f(\alpha_q) >$ is a function of $< \alpha_q >$ that is concave downwards, (ii) has a peak at $< \alpha_0 >$, and (iii) the straight line $< f(\alpha_q) >=< \alpha_q >$ tangentially touches both the spectra around $< \alpha_1 >$, because $< f(\alpha_1) >=< \alpha_1 >$ and $< f'(\alpha_1) >= 1$. The region above the $< f(\alpha_q) >=< \alpha_q >$ line corresponds to an unphysical region. The fact that a wide distribution in $< f(\alpha_q) >$ and not a delta function peaked around α_0 has been

obtained, confirms multifractal nature of the density fluctuation in each case. The left and right sides of the spectrum correspond, respectively, to the dense and sparse regions of density distribution. Both experimental and simulated maximum values of $< f(\alpha_q) >$ are very close to unity, indicating that the empty bin effect particularly in the higher resolution region, is marginal in the present case. The FRITIOF simulated spectrum is wider than the experimental one. For a $p\overline{p}$ interaction similar feature has been observed while UA1 data were being compared with GENCL and PYTHIA predictions [4]. In the case of AB interactions multifractal characteristics were observed both in the experimental data as well as in the Monte Carlo predictions based on a simple stochastic model [8].
As the average number of charged particles in our event sample is finite, the G_q moments contain statistical contribution ($G_q{}^{st}$), that can be determined by distributing n_s particles of an event randomly within $0 \leq X_\eta \leq 1$. In the process short range correlation among the particles, if any, is destroyed. The dynamical contribution ($G_q{}^{dyn}$) can then be extracted after eliminating the statistical one. In [11] it has been shown that, for a trivial dynamics the dynamical part of $< \tau_q >$, denoted by $< \tau(q) >^{dyn}$, should be equal to $(q-1)$. Therefore, any deviation in $< \tau(q) >^{dyn}$ from $(q-1)$ should be read as a contribution from nontrivial dynamical contribution. Allowing all three G-moments namely G_q, G_q^{st} and G_q^{dyn} to obey their respective power laws, the following relation can be obtained,

$$< \tau(q) >^{dyn} =< \tau(q) > - < \tau(q) >^{st} + q - 1. \tag{4.7}$$

whereas, the intermittency index ϕ_q introduced in Eq. (4.1), can also be connected to $< \tau(q) >^{dyn}$ as [11],

$$< \tau(q) >^{dyn} - q + 1 \approx -\phi_q. \tag{4.8}$$

For comparison, ϕ_q values obtained previously from intermittency analysis [10] for the same set of experimental data along with the $(q - 1 - < \tau(q) >)$ and $(q - 1 - < \tau(q) >^{dyn})$ values obtained from the present analysis, are plotted together against q in Fig. 4.3(a). One can see that the ϕ_q values differ from the respective $(q - 1 - < \tau(q) >^{dyn})$ values only to a small extent. The difference in their values may probably be attributed to the different ways of defining SFM and G-moment. The generalized Renyi dimensions denoted by D_q, are directly related to the intermittency indexes as,

$$D_q = 1 - \frac{\phi_q}{(q-1)}. \tag{4.9}$$

Therefore, in view of Eq. (4.8) one can also set,

$$D_q \approx \frac{< \tau(q) >^{dyn}}{(q-1)}. \tag{4.10}$$

On the other hand, the anomalous dimensions are defined as

$$d_q = D - D_q,$$

where D is the topological dimension of the supporting space. For one dimensional analysis $D = 1$. One of the properties of universal multifractals is that, they can be classified by a parameter μ ($0 \leq \mu \leq 2$) called the Levy index, that indicates the degree of multifractality as well as estimates the cascading rate in self-similar branching process [15]. The Levy index (μ) can also be utilized to decipher possible mechanism of particle production. Such a characterization of multifractality is possible if the underlying density distribution can be described by a Levy stable law. Under a Levy law approximation, using anomalous dimensions one can determine the value of μ from the following relation [16],

$$\frac{d_q}{d_2} = \frac{1}{2^\mu - 2}\frac{q^\mu - q}{q-1}. \tag{4.11}$$

In Fig. 4.3(b) experimentally obtained values of d_q/d_2 obtained both from the exact [10] and the approximate values of ϕ_q [Eq. (4.8)], have been plotted together against q. Corresponding d_q/d_2 values evaluated by using Eq. (4.11) have also been incorporated in the same diagram in the form of continuous lines. The lines correspond, respectively, to $\mu = 1.15$ for the exact values of ϕ_q and to $\mu = 1.25$ for the approximate values. If μ were equal to 2, the Levy distribution would have transformed into a Gaussian one. Under this condition one expects minimum fluctuation in the self-similar branching processes. On the other hand, for $\mu = 0$, d_q/d_2 values become independent of order. This corresponds to mono-fractals and maximum fluctuation, and might therefore, be a signal of second order phase transition. Neither of the above conditions is satisfied by the μ values obtained in the present investigation. One can see that, the present values obtained from two different sets of parameters, are very close to each other. The fact that $\mu > 1.0$, indicates presence of wild singularities arising out of non-Poisson like fluctuations in the density distribution. As far as mechanism of particle production is concerned, this condition also indicates that, in the present case of ^{32}S-Ag/Br interactions there may be a non-thermal

phase transition during the cascading process. On the other hand, a value of $0 < \mu < 1.0$ would have indicated soft bound singularities, that can be related to a thermal phase transition interspersed in the cascading process. It should however be mentioned that, the present values of Levy index are less than a previously obtained value ($\mu = 1.6$) based on a set of combined data on AB, pA, e^+e^- and μp interactions [16], but are well within the limit allowed by the Levy law description, and do not necessarily warrant a thermal phase transition to occur during particle production.

4.3 Takagi's Multifractal Moments

As mentioned above, due to the finiteness in charged particle multiplicity (n_s) of an event, the mathematical limit of phase-space partition number ($M \rightarrow \infty$) can not be realised in practice. Even the step function Θ introduced into the definition of the G_q moments, can not completely remove the saturation effects, particularly at higher $|q|$ values as has already been observed. In an alternative approach, Takagi [12] has suggested a new set of multiplicity moments for $q > 0$ as,

$$T_q(\delta X_\eta) = \ln \sum_{i=1}^{N_{ev}} \sum_{j=1}^{M} (p_{ij})^q, \tag{4.12}$$

that are not affected by the finiteness of n_s. Here, $p_{ij}(= n_{ij}/K)$ is the normalized density function, K is the total number of particles produced in N_{ev} interactions and n_{ij} is same as Eq. (4.4), when the entire X_η space has been divided into M intervals. Takagi's method is based on two assumptions, (i) the density function ρ is uniform over the phase-space interval considered, and (ii) the multiplicity distribution P_n does not depend on the location of the interval δX_η - both found to be valid in the present case where X_η has been used as phase-space variable. According to the theory of multifractals, $T_q(\delta X_\eta)$ should be a linear function of the logarithm of the resolution $R(\delta X_\eta)$,

$$T_q(\delta X_\eta) = A_q + B_q \ln R(\delta X_\eta), \tag{4.13}$$

where A_q and B_q are constants independent of q. When a linear dependence like that of Eq. (4.13) is observed over a large range of $R(\delta X_\eta)$, following Takagi's method the generalized dimensions can once again be calculated,

$$D_q = B_q/(q-1). \tag{4.14}$$

For $q = 1$, one may either take the appropriate limit [17], or can consider the entropy function defined as,

$$S(\delta X_\eta) = -\sum_{i=1}^{N_{ev}} \sum_{j=1}^{M} p_{ij} \ln p_{ij}, \tag{4.15}$$

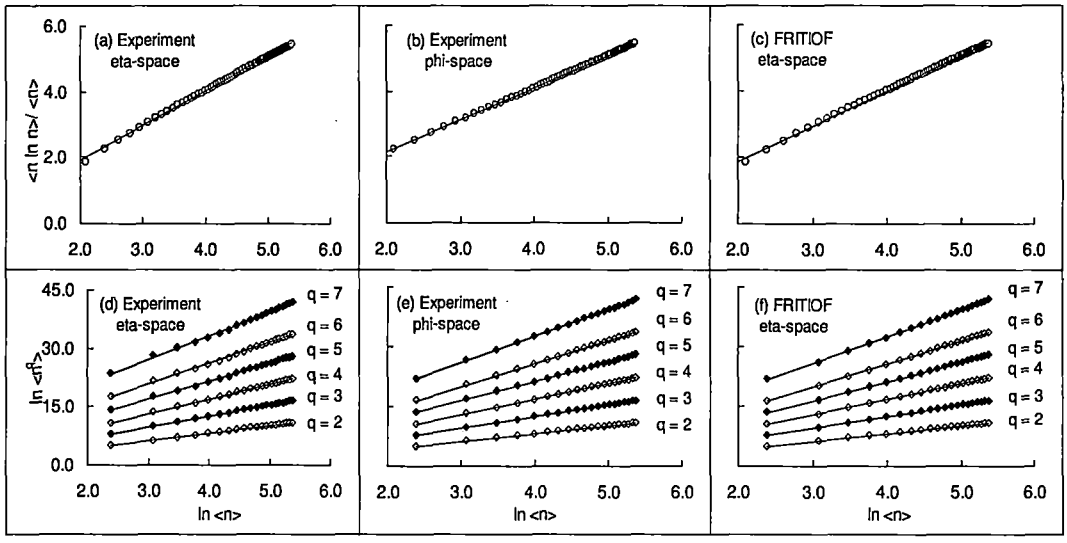

Figure 4.4: Plot of Takagi's multifractal moments for ^{32}S-Ag/Br interaction at 200A GeV/c. In all diagrams the straight lines represent best linear fit to data.

and look for a dependence of this quantity like,

$$S(\delta X_\eta) = -D_1 \ln R(\delta X_\eta) + \text{constant}, \tag{4.16}$$

where D_1 is called the information dimension. If the number of events N_{ev} is large one has,

$$\sum_{i=1}^{N_{ev}} \sum_{j=1}^{M} (p_{ij})^q = < n^q > /(K^{q-1} < n >), \tag{4.17}$$

where average bin multiplicity $< n >= K/(M.N_{ev})$, and therefore,

$$\ln < n_q >= A_q + [(q-1)D_q + 1] \ln(\delta X_\eta) \tag{4.18}$$

for the simplest choice of $R(\delta X_\eta) = \delta X_\eta$. Replacing δX_η with $< n >$, the generalized dimensions can now be obtained following the relations,

$$\ln < n^q >= A_q + [(q-1)D_q + 1] \ln < n > \tag{4.19}$$

for $q \geq 2$. For $q = 1$,

$$< n \ln n > / < n >= C_1 + D_1 \ln < n > . \tag{4.20}$$

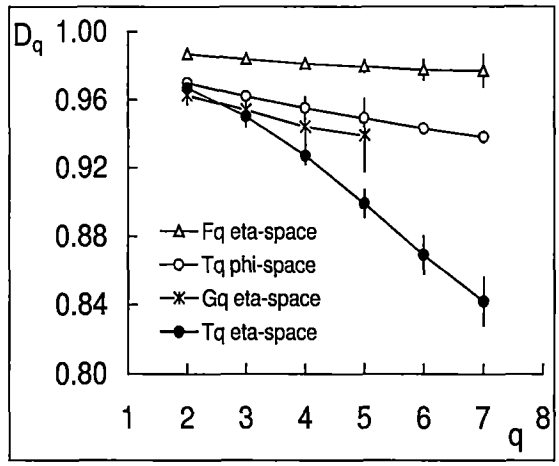

Figure 4.5: Experimental values of the generalised dimensions D_q for ^{32}S-Ag/Br interaction at 200A GeV/c. Solid lines are drawn to guide the eye.

Proceeding in the same way as [12], for a symmetric interval about the central value $X_\eta = 0.5$ of the distribution, values of $< n \ln n >$ and $\ln < n^q >$ are calculated with increasing width of the interval. Our results on Takagi's method of multifractal analysis have been graphically shown by plotting $< n \ln n > / < n >$ against $\ln < n >$, in Fig. 4.4(a)-(c), respectively for the experimental values in η and φ-space and the FRITIOF prediction in η-space. From the slopes of best linear fit to data values of the information dimension (D_1) have been obtained respectively as, $D_1 = 0.973 \pm 0.0014$, 0.972 ± 0.002 and 0.979 ± 002. Values of generalized dimensions for $q \geq 2$ have been obtained from the best linear fit of $\ln < n^q >$ values against $\ln < n >$ as shown in Fig. 4.4(d)-(f). For comparison in Fig. 4.5, D_q values of different orders obtained from Takagi's generalized moments are plotted against q (≥ 2) together with those obtained from the intermittency indexes (ϕ_q) and from the dynamical part of Hwa's multifractal mass exponents $< \tau(q) >^{dyn}$, respectively, making use of Eq. (4.9) and (4.10). With increasing q in general we find a monotonous deceasing trend in the D_q values. However, the D_q values from Takagi's method exhibit steepest fall, whereas those obtained from the intermittency indices decrease at the slowest rate. Probably because of the different ways of defining the multifractal T-moments, and

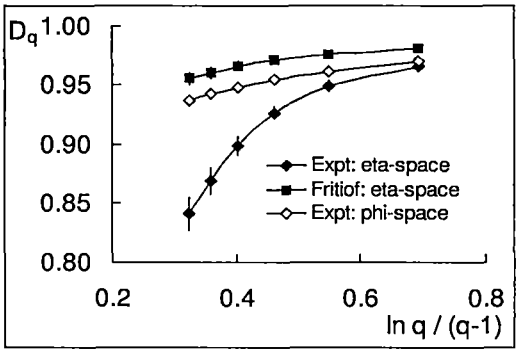

Figure 4.6: Graph to determine the multifractal specific heat for ^{32}S-Ag/Br interaction at 200A GeV/c, from the D_q values obtained by using Takagi's method. The experimental data points in η-space are simply connected by a continuous line, whereas, for both the FRITIOF prediction in η-space and the experimental data points in φ-space, the straight lines represent best linear fit.

due to the reason that in Takagi's method no attempt has been made to separate the non-statistical contribution from the statistical one, in this case at large q the D_q values differ significantly from those obtained from the SFMs and G-moments. However, for a simple Poissonian multiplicity distribution within a given interval δX_η, the D_q values would all have been equal to unity. Any deviation in their values from 1.0 would thus provide us with a measure of nonstatistical fluctuation. This has been found in all the methods described above for characterizing multifractality in density fluctuations. On the basis of the fact that, only Bernoulli type of fluctuations are responsible for a transition from monofractality to multifractality, Bershadskii [18] gave a thermodynamic interpretation of the observed results in terms of a constant specific heat C,

$$D_q = D_\infty + \frac{C \ln q}{q-1}. \tag{4.21}$$

A monofractal to multifractal phase transition corresponds to a jump in the value of C from $C = 0$ to a nonzero finite positive value. By plotting D_q against $\ln q/(q-1)$ we can therefore, obtain the value of specific heat from the slope of the best linear fit. Such a plot can be found in Fig. 4.6 both for the experiment and FRITIOF simulated values. In X_η space a strict linearity is not seen over the entire range of q under consideration, and a linear fit in the range $q = 2\,\text{to}\,5$ resulted into $C = 0.329 \pm 0.061 \approx \frac{1}{3}$. On the other hand best linear fit of FRITIOF data in X_η space over $q = 2\,\text{to}\,7$ results in $C = 0.066 \pm 0.009$,

which is much smaller than the corresponding experimental value. On the other hand, in X_φ space linear fit once again over the entire range of q (= 2 to 7) gave us a much smaller value of $C(= 0.086 \pm 0.008)$. The C value in X_φ space is significantly smaller than a previously obtained value ($C = \frac{1}{4}$) based on an analysis in the azimuthal angle space of similar ^{32}S-ion induced experiment at same incident energy [19]. As a probable reason for this discrepancy, it may be pointed out that the analysis presented in [19] has been performed over a set of events with minimum bias, that possesses a much wider range of impact parameter values, and also has a much smaller average value of shower multiplicity as well as smaller statistics than the present set of experimental data. Our value of C in φ-space is also smaller than the predictions of another analysis ($C = 0.56$) on simulated high multiplicity single jet events in the azimuthal angle space [20].

4.4 Discussion

Observations of the present investigation can be summarized in the following way. From the above analysis of angular distribution of produced particles in ^{32}S-Ag/Br interactions at 200A GeV/c, multifractal characteristics of the density fluctuation over and above that coming from trivial statistical noise, have been established. Results obtained from two different methods of analysis, one prescribed by Hwa [1–3, 11] and the other by Takagi [12], are more or less consistent with each other. However, multifractal nature of the density fluctuation has also been observed in the FRITIOF simulated data. This is in contrast to our previous investigation of intermittency phenomenon for the same set of experimental data [10], where FRITIOF failed to reproduce the experimental observations. The SFM contains information on particle correlation, that has not been taken into account in the present version of FRITIOF. Hence the discrepancy with the experiment has been found. Using Hwa's methodology, not only have we obtained important multifractal parameters like the generalised Renyi dimensions (D_q) and stable multifractal spectrum $f(\alpha_q)$, but also we have been able to determine the Levy index that measures the degree of multifractality for the present set of data on AB interactions. Our value of $\mu(\approx 1.2)$ is consistent with the Levy law description of density distribution of produced charged particles, and also indicates a non-thermal phase transition during particle production. The Takagi's

methodology, perceived to be a better tool of analysis than Hwa's G-moments, once again has been able to establish the multifractal characteristics and yields generalised dimensions. The experimental D_q values obtained from Takagi's method differ significantly from unity with increasing q, whereas, the corresponding FRITIOF values are always very close to unity, which is the topological dimension of the supporting space. The multifractal specific heat, which again is a measure of the degree of multifractality, came out to be higher in pseudorapidity space than the universal value $C = \frac{1}{4}$ for moderate and very heavy-ion interactions, as claimed in [18]. The difference in bias while choosing each experimental data set, should be kept in mind while comparing such parameter values obtained from different investigations. A small FRITIOF simulated value of C indicates that, though mulitfractal characteristics are present also in the simulated events, the extent of multifractality is smaller than that of the experimental one. In the azimuthal angle space, in contrast to some previous observations, present value of C came out to be substantially smaller.

We would like to point out that several measures can be taken, to enable us in future to make stronger conclusions. First of all, fractal structures present in higher dimensions is a worthwhile topic of future investigation. Often self-similar multifractal characteristics of geometrical objects disappear in their lower dimensional projection, and therefore, stronger indication of multifractality is expected in a higher dimensional analysis. The influence of collision geometry can be another aspect that requires special attention, when a much larger statistics is available. This requires partitioning the data set into several subsets, each with a narrow range of shower multiplicity. Performing similar multifractal analysis for each such subset, variation with $< n_s >$ (a measure of impact parameter of collision) can be examined. The fact that FRITIOF simulated events also exhibit multifractality while it fails to do so in the case of intermittency, is a major point of concern. More sophisticated methods of analysis are therefore necessary, where the structure obtained from trivial backgrounds can be properly accounted for. The generalized dimensions obtained from Takagi's methodology are significantly different in the higher q region, from similar values obtained from the SFM and G-moment analysis of data. This discrepancy probably arises because, in Takagi's method the issue of eliminating statistical noise has not yet been addressed.

Bibliography

[1] R. C. Hwa, *Phys. Rev.* **D 41,** 1456 (1990).

[2] W. Florkowski and R. C. Hwa, *Phys. Rev.* **D 43,** 1548 (1991).

[3] C. B. Chiu and R. C. Hwa *Phys. Rev.* **D 43,** 100 (1991).

[4] UA1 Collaboration, C. Albajar, *et al.*, *Z. Phys.* **C 56,** 37 (1991).

[5] I. Derado, R. C. Hwa, G. Jansco and N. Schmitz *Phys. Lett.* **B 283,** 151 (1991).

[6] R. K. Shivpuri and V. Anand, *Phys. Rev.* **D 50,** 287 (1994).

[7] E. K. Sarkisyan, L. K. Gelovani and G. G. Taran, *Phys. Lett.* **B 302,** 331 (1993).

[8] EMU01 Collaboration, M. I. Adamovich *et al.*, *Europhys. Lett.* **44,** 571 (1998).

[9] E. A. De Wolf, I. M. Dremin and W. Kittel, *Phys. Rep.* **270** 1 (1996); W. Kittel and E. A. De Wolf, *Soft Multihadron Dynamics*, (World Scientific, Singapore), (2005).

[10] M. K. Ghosh, A. Mukhopadhyay and G. Singh, *J. Phys. G: Nucl. Part. Phys.* **34,** 177 (2007).

[11] R. C. Hwa and J. Pan, *Phys. Rev.* **D 45,** 1476 (1992).

[12] F. Takagi *Phys. Rev. Lett.* **72,** 32 (1994).

[13] B. Anderson, G. Gustavson and B. Nilsson-Almqvist, *Nucl. Phys.* **B 281,** 289 (1987) B. Nilsson-Almquist and E. Stenlund, *Comp. Phys. Commun.* **43,** 387 (1987).

[14] A. Bialas and M. Gradzicki *Phys. Lett.* **B 252,** 483 (1990).

[15] Ph. Brax and R. Peschanski, *Phys. Lett.* **B 253,** 225 (1991).

[16] W. Ochs *Phys. Lett.* **B 247,** 101 (1990).
W. Ochs *Z. Phys.* **C 50,** 339 (1991).

[17] H. G. E. Hentschel and I. Proccacia *Physica* **D 40,** 435 (1983).

[18] A. Bershadskii, *Phys. Rev.* **C 59,** 364 (1999).

[19] D. Ghosh *et al.*, *Z. Phys.* **C 73,** 269 (1997).

[20] S. K. Nayak and Y. P. Viyogi *Phys. Lett.* **B 367,** 386 (1996).